

1 **Supporting Information**

2

3

4 **Enhanced Thermal Conductive Property of Polyamide**
5 **Composites by Low Mass Fraction of Covalently-Grafted**
6 **Graphene Nanoribbons**

7

8 Peng Ding ^{a*}, Nan Zhuang ^a, Xieliang Cui ^b, Liyi Shi ^a, Na Song ^a, Shengfu Tang ^a

9 ^a Research Center of Nanoscience and Nanotechnology, Shanghai University, 99

10 Shangda Road, Shanghai 200444, PR China

11 ^b Department of Polymer Materials, Shanghai University, 99 Shangda Road, Shanghai

12 200444, PR China

13

14

15

16

17

18

19

20

21

* Corresponding author. Tel/Fax: +86 21-66134726. E-mail address: dingpeng@shu.edu.cn (P. Ding)

1

2 1) The detailed test procedure of thermal conductivity (λ) in the through-plane and in-plane
3 directions

4 2) Fig. S1 – Experimental diagram

5 3) Fig. S2 – TGA analysis of CNT, GNR, PA6, and PGR composites

6 4) Fig. S3 – TEM images of PGR-0.1

7 5) Fig. S4 Test for intrinsic viscosity and molecular weight for PA6 and PGR.

8 6) Table S1 The η_{in} of free PA6 in PGR composites.

9 7) Fig. S5 – TEM images of PGR-0.7

10 8) Fig. S6 – SEM images of PGR composites

11 9) Table S2: A comprehensive comparison on the improvement in thermal conductivities of
12 nanocomposites with different types of fillers

13

1 **The detailed test procedure of thermal conductivity (λ) in the through-plane and in-plane**

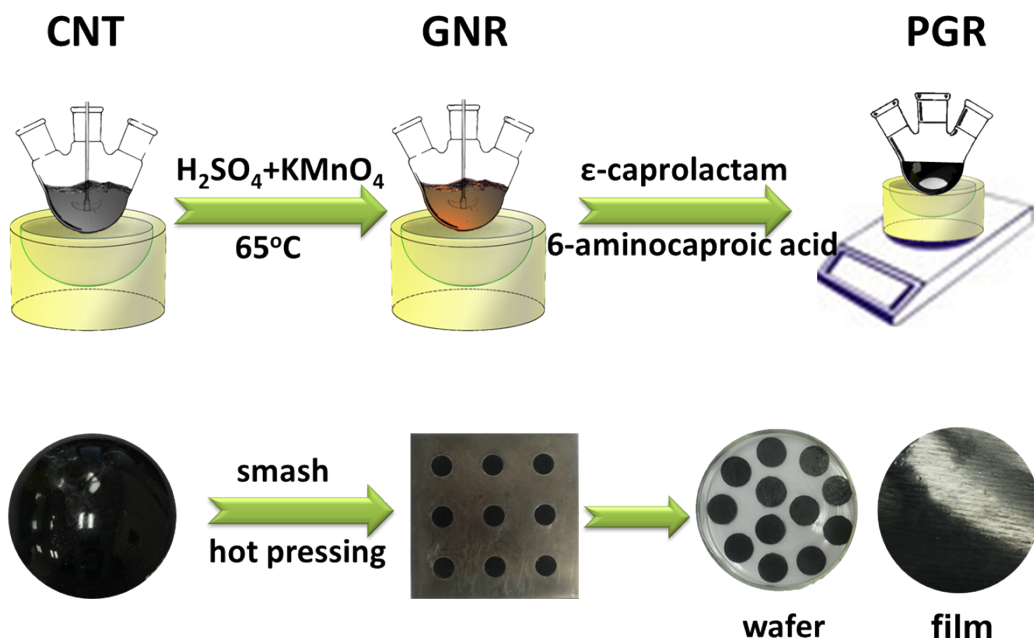
2 **directions**

3 The laser flash technique has been generally known as the standard and the popular method for
4 measuring thermal diffusivities of solid materials above room temperature. The thermal
5 conductivity (λ) of the composites was measured by the transient laser flash technique with the
6 Netzsch LFA 447 Nanoflash at 25 °C according to ASTM E1461 standard (“Compos. Sci. Technol.
7 2014; 90: 123”, “Compos. Sci. Technol. 2014; 94: 147”, “Compos. Sci. Technol. 2010; 70: 2176”,
8 “J. Mater. Sci. 2014; 49: 5256”, “Carbon. 2012; 50 (14): 5052” and “Fiber. Polym. 2013; 14: 1317”).
9 The transient laser flash technique uses a xenon flash lamp to heat the sample from one side by
10 producing shots with energy of 10 J/pulse. The temperature rise was determined at the back side
11 with the nitrogen-cooled InSb IR detector. The output of the temperature detector was amplified
12 and adjusted for the initial ambient conditions. The recorded temperature rise curve was the change
13 in the sample temperature resulting from the firing of the flash lamp. The magnitude of the
14 temperature rise and the amount of the light energy were not required for a diffusivity determination;
15 only the shape of the curve was used in the analysis. From the analysis of the resulting relative
16 temperature (T/T_{peak})-time curve, the thermal diffusivity (α) can be obtained. For the specific heat
17 (C_p) measurement, the magnitude of the temperature rise of an unknown sample was compared to
18 that of the reference calibration sample which we used pyrex in the direction of through-plane
19 testing. λ was calculated from the equation: $\lambda(T) = \alpha(T)C_p(T)\rho(T)$ (where ρ is the density of the
20 composites and can be obtained from the density measurement through a density balance). λ had
21 been revised in the calculation process. The C_p of samples was a relative value which relative to the
22 C_p of the reference calibration sample. To keep the good contact interface between the samples and
23 the probe of Nanoflash, the surfaces of sample disks generally needed to be polished with abrasive

1 paper, though most of them were already flat after hot-pressing. Moreover, before the λ
2 measurement, both sides of each disks needed to be sprayed a layer of graphite to reduce the laser
3 scattering by the initial surfaces of samples. In addition, the thermal conductivity of each
4 temperature point needed to be measured for at least three times, and the average value was the final
5 result.

6 In this method, the samples with different shapes and sizes are necessary for testing the thermal
7 conductive properties in in-plane and through-plane directions. For through-plane direction, the
8 diameter and thickness were 12.7 and 1.0 mm, respectively. But for in plane direction, the diameter
9 and thickness were 25 and 0.1 mm, respectively.

10

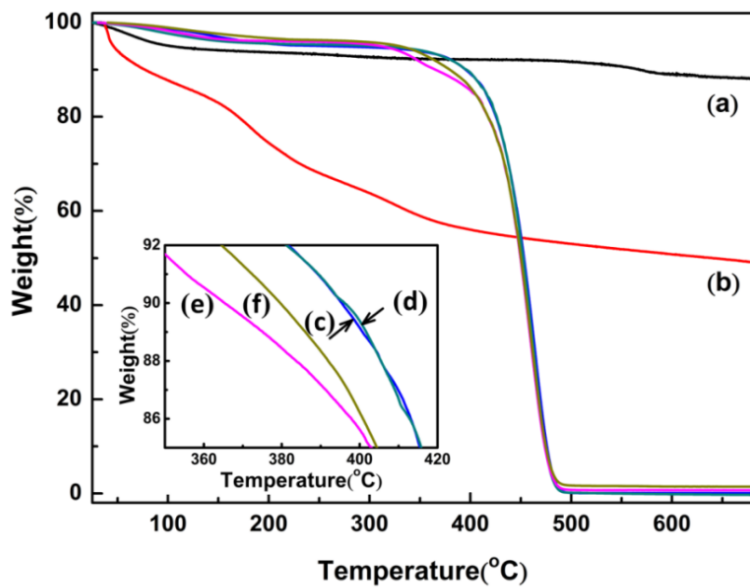


11

12

Fig. S1 Experimental diagram

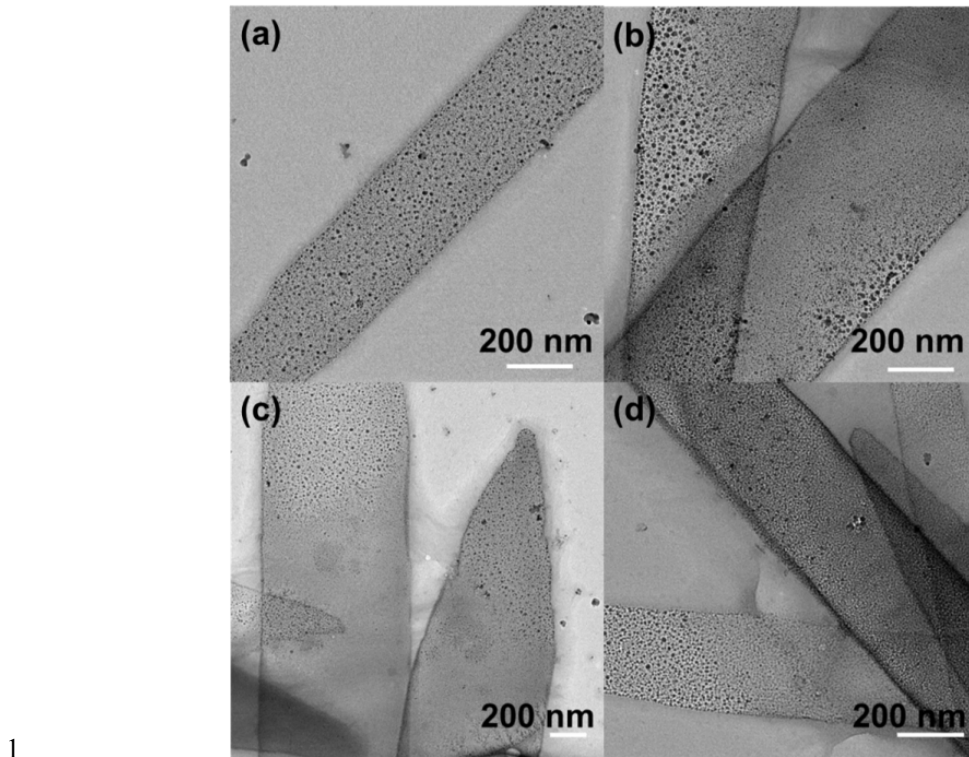
13



1

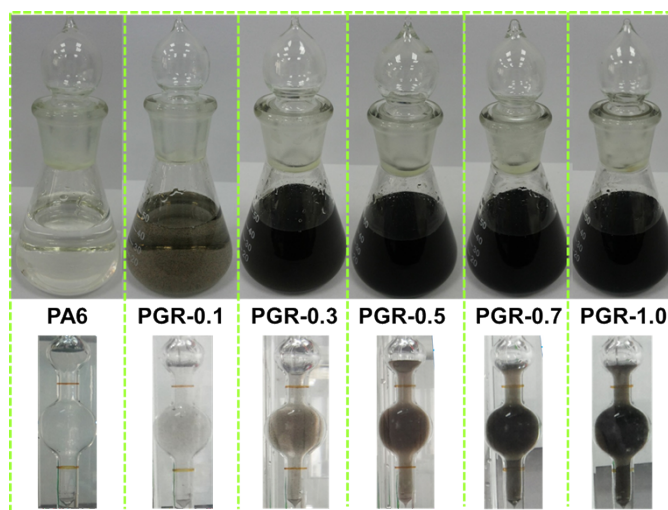
2 **Fig. S2 TGA analysis of (a)CNT, (b)GNR, (c)PA6, (d)PGR-0.1, (e)PGR-0.5 and (f) PGR-1.0.**

3 Thermogravimetric analysis and differential scanning calorimetry measurements were applied
 4 to study the thermal properties of the PGR composites. The TGA thermograms of pure PA6 and
 5 PGR composites were obtained under a nitrogen atmosphere. From Figure S2, there are more
 6 oxygen-containing functional groups on the surface and edges of GNR than CNT (weight loss of
 7 50% and 10%, respectively). However there are little differences between TGA curves of PGR
 8 composites (PGR-0.1, PGR-0.5, PGR-1.0) and PA6, on account of the extremely low GNR wt.%
 9 including oxygen-containing groups have been grafted to the PA6 chains after thermal reduction
 10 progress at 250 °C.



2 **Fig. S3 TEM images of PGR-0.1.**

3 PGR-0.1 samples were dissolved in formic acid with a concentration of 0.5 mg/mL and then
4 sonicated for 5 min.

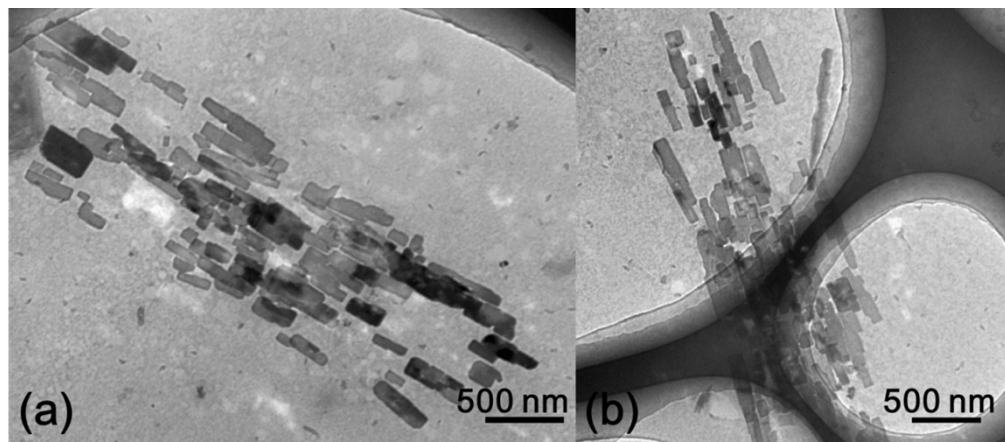


5 **Fig. S4 Test for intrinsic viscosity and molecular weight for PA6 and PGR.**

Sample	PA6	PGR-0.1	PGR-0.3	PGR-0.5	PGR-0.7	PGR-1.0
η_{in} (mL.g ⁻¹)	120.8	93.3	66.1	43.6	82.3	85.7

7 **Table S1 The η_{in} of free PA6 in PGR composites.**

1



2

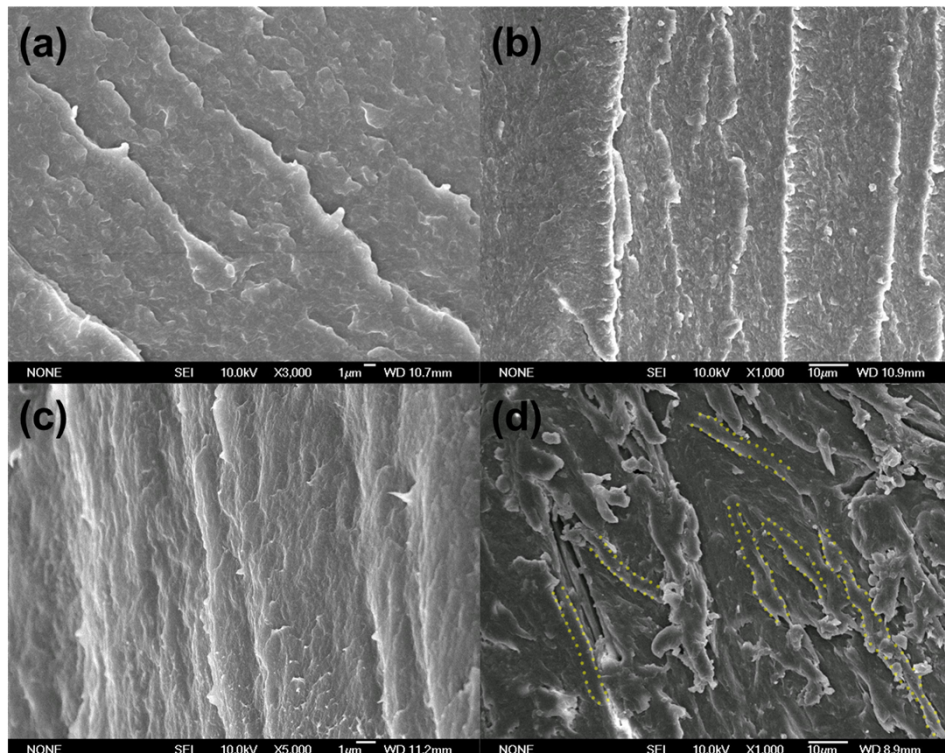
3

Fig. S5 TEM images of PGR-0.7.

4

PGR-0.7 samples were cutting into ultrathin sections, and loaded to a copper network.

5



6

Fig. S6 SEM images of PGR-0.1 (a), PGR-0.5 (b), PGR-0.7 (c) and PGR-1.0 (d).

7

Samples were frozen in liquid nitrogen for 10 min and then clamped off with pliers to observe the fracture surface morphologies.

8

9

10

1 **Table S2: Comprehensive comparison on the improvement in thermal conductivities of**
 2 **nanocomposites with different types of fillers**
 3

	Ref.	Matrix	Type of filler	TC of matrix λ_0 (W·m ⁻¹ K ⁻¹)	Thermal Conductivity			$\lambda'/\text{wt. \%}$
					λ_{\perp} (W·m ⁻¹ K ⁻¹)	Filler content	λ' (λ/λ_0)	
Thermal plastic polymer matrix	1	PA66	CF	0.3	0.44	20 wt.%	1.5	7.5
	2	PA66	CF	0.25	0.95	40 wt.%	3.8	9.5
					0.327	5 wt.%	1.3	26.2
	3	PA6	Graphite/CF	0.13	0.3	30 wt.% (no CF)	2.3	7.7
					2.05	60 wt.% (30wt.% CF)	15.8	26.3
	4	PA6	Copper plates	0.3	11.57	92.2 wt.%	38.6	41.9
	5	PA6	Glass fiber/CNT	0.041	0.058	2 wt.%	1.4	70
	6	PA66	Glass fiber/carbon black/graphite	0.25	0.7	30 wt.%	2.8	9.3
	7	PA66	Carbon black	0.3	1.142	30 wt.%	3.8	12.7
	8	PA6	Expandable Graphite	NA	1.965	15 wt.%	7	47
					32.33	70 wt.%	110	157
	9	PA66	Graphite	0.278	1.219	40 wt.%	4.4	10.9
			CF		1.034		3.7	9.3
	10	PA	OMMT	0.127	≈0.135	5 wt.%	1.1	21.3
	11	PA11	MWNT	NA	≈0.27	5 wt.%	NA	NA
	12	PA6	CF/Al ₂ O ₃ /Mg(OH) ₂ /graphite	0.27	2.1	50 wt.%	7.8	15.6
	13	PA6	LTEG	0.2939	21.05	60 wt.%	71.6	119.4
	14	PA6	CF	0.21	0.32	30 wt.%	1.5	5.1
	15	PA6	CF/BN	0.25	0.98	20 vol.%	3.9	19.6
	16	PA6	Fe ₃ O ₄	0.22	0.93	47 vol.%	4.2	8.9
	17	PA11	CF	0.24	0.3	7.5 wt.%	1.3	16.7
	18	PA6	OMMT	0.28	0.45	20 wt.%	1.6	8
	19	PA6	MWCNT	0.33	0.42	2.1 wt.%	1.3	60.6
	20	PA6/P C(7/3)	Flake graphite	0.292	4.754	50 wt.%	16.3	32.6
	21	PA66/polycarbonate	Carbon black	0.3	1.1	40 wt.%	3.7	9.2

22	PAI	MWCNT	0.76	1.41	1.0 wt.%	1.9	190
23	PS	MWCNT/C foam	0.12	0.32	20 wt.%	2.7	13.3
				0.17	1 wt.%	1.4	141.7
24	PS	SWCNTs	0.133	0.62	30 wt.%	4.7	15.6
				0.36	5 wt.%	2.7	54.1
25	PS	MWNT-g-SMA	0.18	0.89	35 vol.%	4.9	NA
				≈0.2	2.5 vol.%	1.1	NA
26	PC	CNT	0.218	0.306	8 wt.%	1.4	17.6
				0.232	2 wt.%	1.1	53.2
27	PC	GNP	0.215	0.489	15 wt.%	2.3	15.2
				0.251	2 wt.%	1.2	58.4
28	PC	u-MWCNT	0.2	0.28	2.5 wt.%	1.4	56
29	HDPE	Branch- structured nickel	0.468	1.99	30 vol.%	4.3	NA
30	Bio- based polyest er	Graphene oxide	0.19	0.542	1.45vol. %	2.9	NA
31	PP	Graphite	~0.22	≈0.5	20 wt.%	2.3	11.4
				≈0.2	2 wt.%	0.9	45.5
32	PP	Synthetic graphite	0.20	6.042	80 wt.%	30.2	37.8
		CNT		0.467	15 wt.%	2.3	15.6
33	PP	CB/CNT/SG	0.206	0.36	15 wt.%	1.7	11.4
				0.5	15 wt.%	2.4	15.9
				9.47	80 wt.%	45.1	56.4
34	PP	SG/CB/CNT	0.21	9.47	80 wt.%	45.1	56.4
				0.36	15 wt.%	1.7	11.4
				0.5	15 wt.%	2.4	15.9
35	PP	GNP	~0.25	1.2	25 vol.%	4.8	19.2
36	EVA	ZnO	0.25	≈0.78	27 vol.%	3.1	NA
37	LCP	Graphite	0.4	28.3	70 wt.%	70.8	101.1
38	LCP	Carbon black	1	2.06	15 wt.%	2.1	13.7
		Synthetic graphite		4.33	40 wt.%	4.3	10.8
		CF		2.49	60 wt.%	2.5	4.2
39	LCP	Graphite	0.22	2.624	75 wt.%	11.9	15.9
40	LCP	Carbon black	0.22	2.63	75 wt.%	12	15.9
41	polysil oxane	BN nanosheets	0.086	0.127	5 wt.%	1.5	30
Our previous	PA6	Graphene oxide	0.196	0.416	10 wt.%	2.1	21.2

work ⁴²								
This work	PA6	GNR	0.21	0.41	0.5 wt.%	1.952	390.5 (λ_{\perp})	
			1.83	4.85		2.654	530.8 ($\lambda_{//}$)	
Thermal set polymer matrix	43	epoxy	GNPs	0.195	5.864 0.303	20 wt.% 2 wt.%	28 1.6	140 77.7
	44	epoxy	SiC-HBP	0.167	\approx 0.334	30 wt.%	2	6.7
	45	epoxy	Al ₂ O ₃	0.236	0.4	20 wt.%	1.7	8.5
	46	epoxy	BN	0.258	0.265	5 wt.%	1.03	20.5
			BN-ODA		0.31	5 wt.%	1.2	24
			BN-HBP		0.329	5 wt.%	1.28	25.5
	47	epoxy	BN and Al ₂ O ₃	0.188	0.808	26.5 vol.%	4.3	16.2
	48	epoxy	GNP	\sim 0.212	0.72	2.7 vol.%	3.4	NA
					0.35	0.5 vol.%	1.7	NA
	49	epoxy	MWCNT	0.242	0.251	0.3 wt.%	1	345.7
	50	epoxy	MWCNT	\sim 0.12	\approx 0.25	1.5 wt.%	2.1	138.9
					0.21	0.5 wt.%	1.8	350
	51	epoxy	Al ₂ O ₃ -CNTs	\sim 0.17	0.4	0.75 wt.%	2.4	320
						(CNT: 0.15 wt.%)		
1	52	epoxy	GNP-SWCNT	-	1.75	10 wt.%	\sim 8.0	80
2	53	S160	Aligned CNT	0.56	1.21	0.3 vol.%	2.2	733.3
3	54	FKM	Aligned CNT	0.21	23.3	13.2 wt.%	109.9	832.6

1

2 *LTEG, PC, CF, SMA, GNP, S160, and FKM represent: low temperature of expandable
 3 graphite, polycarbonate, carbon fiber, poly(styrene-co-maleic anhydride), graphite nanoplatelet,
 4 silicone elastomer (Sylard 160, Dow Corning) , and fluorinated rubber, respectively.

Reference

1. J. A. Heiser and J. A. King, *Polym. Compos.*, 2004, **25**, 186-193.
2. M. G. Miller, J. M. Keith, J. A. King, R. A. Hauser and A. M. Moran, *J. Appl. Polym. Sci.*, 2006, **99**, 2144-2151.
3. Y. Yoo, H. L. Lee, S. M. Ha, B. K. Jeon, J. C. Won and S. G. Lee, *Polym. Int.*, 2014, **63**, 151-157.
4. H. S. Tekce, D. Kumlutas and I. H. Tavman, *J. Reinforced Plast. Compos.*, 2007, **26**, 113-121.
5. Z. Q. Shen, S. Bateman, D. Y. Wu, P. McMahon, M. Dell'Olio and J. Gotama, *Compos. Sci. Technol.*, 2009, **69**, 239-244.
6. J. A. King, K. W. Tucker, B. D. Vogt, E. H. Weber and C. L. Quan, *Polym. Compos.*, 1999, **20**, 643-654.
7. J. A. King, K. W. Tucker, J. D. Meyers, E. H. Weber, M. L. Clingerman and K. R. Ambrosius, *Polym. Compos.*, 2001, **22**, 142-154.
8. S. T. Zhou, Y. Z. Lei, H. W. Zou and M. Liang, *Polym. Compos.*, 2013, **34**, 1816-1823.
9. J. M. Keith, C. D. Hingst, M. G. Miller, J. A. King and R. A. Hauser, *Polym. Compos.*, 2006, **27**, 1-7.
10. M. Baniassadi, A. Laachachi, F. Hassouna, F. Addiego, R. Muller, H. Garmestani, S. Ahzi, V. Tonizazzo and D. Ruch, *Compos. Sci. Technol.*, 2011, **71**, 1930-1935.
11. M. Q. Yuan, B. Johnson, J. H. Koo and D. Bourell, *J. Compos Mater.*, 2014, **48**, 1833-1841.
12. M. H. Li, Y. Z. Wan, Z. F. Gao, G. Y. Xiong, X. M. Wang, C. B. Wan and H. L. Luo, *Mater. Des.*, 2013, **51**, 257-261.
13. S. T. Zhou, L. Yu, X. Song, J. Chang, H. W. Zou and M. Liang, *J. Appl. Polym. Sci.*, 2014, **131**, 10.
14. X. L. Yan, Y. Imai, D. Shimamoto and Y. Hotta, *Polymer*, 2014, **55**, 6186-6194.
15. D. Shimamoto, Y. Imai and Y. Hotta, *J. Ceram. Soc. Jpn.*, 2014, **122**, 732-735.
16. B. Weidenfeller, M. Hofer and F. Schilling, *Compos. Pt. A-Appl. Sci. Manuf.*, 2002, **33**, 1041-1053.
17. A. L. Moore, A. T. Cummings, J. M. Jensen, L. Shi and J. H. Koo, *J. Heat Transf.-Trans. ASME*, 2009, **131**, 5.
18. H. Zhou, S. M. Zhang and M. S. Yang, *J. Appl. Polym. Sci.*, 2008, **108**, 3822-3827.
19. J. C. Yu, B. Tonpheng, G. Grobner and O. Andersson, *Carbon*, 2011, **49**, 4858-4866.
20. S. T. Zhou, Y. Chen, H. W. Zou and M. Liang, *Thermochim. Acta*, 2013, **566**, 84-91.
21. E. H. Weber, M. L. Clingerman and J. A. King, *J. Appl. Polym. Sci.*, 2003, **88**, 112-122.
22. S. H. Lee, S. H. Choi, S. Y. Kim and J. R. Youn, *J. Appl. Polym. Sci.*, 2010, **117**, 3170-3180.
23. L. Ji, M. M. Stevens, Y. Zhu, Q. Gong, J. Wu and J. Liang, *Carbon*, 2009, **47**, 2733-2741.
24. J. E. Peters, D. V. Papavassiliou and B. P. Grady, *Macromolecules*, 2008, **41**, 7274-7277.
25. H. Tu and L. Ye, *J. Appl. Polym. Sci.*, 2010, **116**, 2336-2342.
26. J. A. King, M. D. Via, J. A. Caspary, M. M. Jubinski, I. Miskioglu, O. P. Mills and G. R. Bogucki, *J. Appl. Polym. Sci.*, 2010, **118**, 2512-2520.
27. J. A. King, M. D. Via, F. A. Morrison, K. R. Wiese, E. A. Beach, M. J. Cieslinski and G. R. Bogucki, *J. Compos. Mater.* 2012, **46**, 1029-1039.
28. M. Liebscher, T. Gaertner, L. Tzounis, M. Micusik, P. Poetschke, M. Stamm, G. Heinrich and B. Voit, *Compos. Sci. Technol.*, 2014, **101**, 133-138.
29. I. Krupa, V. Cecen, A. Boudenne, J. Prokes and I. Novak, *Mater. Des.*, 2013, **51**, 620-628.

30. Z. H. Tang, H. L. Kang, Z. L. Shen, B. C. Guo, L. Q. Zhang and D. M. Jia, *Macromolecules*, 2012, **45**, 3444-3451.
31. V. Causin, C. Marega, A. Marigo, G. Ferrara and A. Ferraro, *Eur. Polym. J.*, 2006, **42**, 3153-3161.
32. J. A. King, B. A. Johnson, M. D. Via and C. J. Ciarkowski, *Polym. Compos.*, 2010, **31**, 497-506.
33. J. A. King, D. L. Gaxiola, B. A. Johnson and J. M. Keith, *J. Compos Mater.*, 2010, **44**, 839-855.
34. D. L. Gaxiola, J. M. Keith, N. Mo, J. A. King and B. A. Johnson, *J. Compos Mater.*, 2011, **45**, 1271-1284.
35. K. Kalaitzidou, H. Fukushima and L. T. Drzal, *Carbon*, 2007, **45**, 1446-1452.
36. B. Lee and G. Dai, *J. Mater. Sci.*, 2009, **44**, 4848-4855.
37. S. M. Ha, H. L. Lee, S. G. Lee, B. G. Kim, Y. S. Kim, J. C. Won, W. J. Choi, D. C. Lee, J. Kim and Y. Yoo, *Compos. Sci. Technol.*, 2013, **88**, 113-119.
38. T. N. G. Adams, T. R. Olson, J. A. King and J. M. Keith, *Polym. Compos.*, 2011, **32**, 147-157.
39. M. G. Miller, J. M. Keith, J. A. King, B. J. Edwards, N. Klinkenberg and D. A. Schiraldi, *Polym. Compos.*, 2006, **27**, 388-394.
40. J. A. King, R. L. Barton, R. A. Hauser and J. M. Keith, *Polym. Compos.*, 2008, **29**, 421-428.
41. H. B. Cho, Y. Tokoi, S. Tanaka, T. Suzuki, W. H. Jiang, H. Suematsu, K. Niihara and T. Nakayama, *J. Mater. Sci.*, 2011, **46**, 2318-2323.
42. P. Ding, S. S. Su, N. Song, S. F. Tang, Y. M. Liu and L. Y. Shi, *Carbon*, 2014, **66**, 576-584.
43. S. Ganguli, A. K. Roy and D. P. Anderson, *Carbon*, 2008, **46**, 806-817.
44. Z. K. Yuan, J. H. Yu, B. L. Rao, H. Bai, N. Jiang, J. Gao and S. R. Lu, *Macromol. Res.*, 2014, **22**, 405-411.
45. J. H. Yu, X. Y. Huang, L. C. Wang, P. Peng, C. Wu, X. F. Wu and P. K. Jiang, *Polym. Chem.*, 2011, **2**, 1380-1388.
46. J. H. Yu, X. Y. Huang, C. Wu, X. F. Wu, G. L. Wang and P. K. Jiang, *Polymer*, 2012, **53**, 471-480.
47. L. J. Fang, C. Wu, R. Qian, L. Y. Xie, K. Yang and P. K. Jiang, *RSC Adv.*, 2014, **4**, 21010-21017.
48. M. Chao, Y. Demei, C. Jingyu, W. Guolong and F. Lihua, *Carbon*, 2013, **55**, 116-125.
49. F. H. Gojny, M. H. G. Wichmann, B. Fiedler, I. A. Kinloch, W. Bauhofer, A. H. Windle and K. Schulte, *Polymer*, 2006, **47**, 2036-2045.
50. Y. S. Song and J. R. Youn, *Carbon*, 2005, **43**, 1378-1385.
51. M. Bozlar, D. He, J. Bai, Y. Chalopin, N. Mingo and S. Volz, *Adv. Mater.*, 2010, **22**, 1654-1658.
52. A. P. Yu, P. Ramesh, X. B. Sun, E. Bekyarova, M. E. Itkis and R. C. Haddon, *Adv. Mater.*, 2008, **20**, 4740-4744.
53. H. Huang, C. H. Liu, Y. Wu and S. S. Fan, *Adv. Mater.*, 2005, **17**, 1656-1661.
54. K. Uetani, S. Ata, S. Tomonoh, T. Yamada, M. Yumura and K. Hata, *Adv. Mater.*, 2014, **26**, 5857-5862.